Available online at www.sciencedirect.com
SCIENCE DIRECT
Biochemical and Biophysical Research Communications 344 (2006) 87–94
BBRC
www.elsevier.com/locate/ybbrc

Nucleic acid-binding properties of the RRM-containing protein RDM1 ☆,☆☆

Samia Hamimes [a], Dominique Bourgeon [a], Alicja Z. Stasiak [b], Andrzej Stasiak [b], Eric Van Dyck [a,*]

[a] *International Agency for Research on Cancer (IARC), 150 Cours Albert Thomas, 69372 Lyon, France*
[b] *Laboratoire d'Analyse Ultrastructurale, Université de Lausanne, 1015 Lausanne, Switzerland*

Received 16 March 2006
Available online 3 April 2006

Abstract

RDM1 (RAD52 Motif 1) is a vertebrate protein involved in the cellular response to the anti-cancer drug cisplatin. In addition to an RNA recognition motif, RDM1 contains a small amino acid motif, named RD motif, which it shares with the recombination and repair protein, RAD52. RDM1 binds to single- and double-stranded DNA, and recognizes DNA distortions induced by cisplatin adducts in vitro. Here, we have performed an in-depth analysis of the nucleic acid-binding properties of RDM1 using gel-shift assays and electron microscopy. We show that RDM1 possesses acidic pH-dependent DNA-binding activity and that it binds RNA as well as DNA, and we present evidence from competition gel-shift experiments that RDM1 may be capable of discrimination between the two nucleic acids. Based on reported studies of RAD52, we have generated an RDM1 variant mutated in its RD motif. We find that the $L_{119}GF \rightarrow AAA$ mutation affects the mode of RDM1 binding to single-stranded DNA.

Keywords: RRM; RDM1; RAD52; Nucleic acid binding; Gel-shift assays; Acidic pH

The RNA recognition motif (RRM) is a single-stranded (ss) nucleic acid-binding domain that is widely distributed amongst living organisms [1,2]. RRMs are about 90 amino acids in size and contain two short, conserved elements, RNP1 and RNP2, involved in ssRNA interaction [3,4]. While RRMs can be found in single copies, very often they are present in multiple copies within a single polypeptide and/or in association with other domains, which contribute to the protein cooperativity and/or affinity for ssRNA [1,5]. Although predominantly found in RNA-binding proteins, RRMs are also endowed with ssDNA-binding properties, and a growing list of proteins has been found to which RRMs confer both ssDNA- and RNA-binding ability [6–8]. In addition, duplex DNA binding by RRM domains has been documented [9–12]. RRM domains have also been shown to mediate protein recognition [13]. RRM-containing proteins display a wide subcellular distribution that reflects a vast spectrum of functions in pre-mRNA processing and splicing, RNA stability, sequestration and degradation, mRNA transport, rRNA metabolism, and telomere metabolism [14,15,23].

We have recently identified a novel RRM-containing protein in vertebrates [16]. Ablation of the *RDM1* gene (for *RAD52Motif 1*) encoding this protein in the chicken B cell line DT40 led to an increased sensitivity to the

☆ This work was partially supported by grants from La Ligue contre le Cancer, Comité du Rhône, and l'Association pour la Recherche sur le Cancer, as well as by Grant 3100A0-103962 from the Swiss National Science Foundation.
☆☆ *Abbreviations:* ds, double-stranded; DSB, double-stranded break; DTT, dithiothreitol; EDTA, ethylenediaminetetraacetic acid; HEPES, *N*-(2-hydroxyethyl)piperazine-*N*′-(2-ethanesulfonic acid); MES, 2-(*N*-morpholino)ethanesulfonic acid; PIPES, piperazine-*N*,*N*′-bis(2-ethanesulfonic acid); RD motif, RAD52 motif; RNP, ribonucleoprotein; RRM, RNA recognition motif; ss, single-stranded; TAE, Tris acetate–EDTA; TBE, Tris borate–EDTA.
* Corresponding author. Fax: +33 4 72 73 83 22.
E-mail address: Vandyck@iarc.fr (E. Van Dyck).

0006-291X/$ - see front matter © 2006 Elsevier Inc. All rights reserved.
doi:10.1016/j.bbrc.2006.03.154

anti-cancer drug cisplatin. With the exception of a single RRM, inspection of the RDM1 protein sequence revealed no putative DNA- or RNA-binding motif [16]. However, adjacent to its RRM, RDM1 was found to contain a stretch of 21 amino acids, named RD motif, conserved in the RAD52 protein involved in homologous recombination and the repair of DNA double-stranded breaks (DSBs) [16–18]. In RAD52, the region comprising this motif plays an important role in ssDNA binding ([20] and references therein), raising the issue of whether the RD motif of RDM1 may contribute to its DNA-binding activity. Using gel-shift assay and electron microscopy, we have shown that purified, recombinant chicken RDM1 protein binds to ssDNA, as well as double-stranded (ds) DNA on which it assembles filament-like structures. RDM1 also recognizes the distortions of the double helix caused by cisplatin-DNA adducts in vitro, suggesting that it may act as a DNA-damage recognition factor [16].

Here, we have carried out a more in-depth analysis of the interaction between RDM1 and nucleic acids. We show that RDM1 protein binds to RNA as well as DNA, and present evidence from binding competition experiments that it may discriminate between its DNA and RNA targets. We also demonstrate that RDM1 displays acidic pH-dependent DNA-binding activity. Finally, based on the documented properties of the RAD52 protein, we have generated an RDM1 variant mutated in its RD motif. We find that the $L_{119}GF \rightarrow AAA$ mutation does not impair the homotypic interactions of RDM1, as detected by the yeast two-hybrid assay. However, gel-shift assays and electron microscopic analyses indicate that this mutation affects the mode of RDM1 binding to ssDNA, suggesting a role for the RD motif in modulating the DNA-binding properties of RDM1.

Materials and methods

Plasmid construction and yeast two-hybrid analysis. The chicken RDM1(119–121 LGF → AAA) mutant was generated by site-directed mutagenesis using the wild-type *RDM1* cDNA [16] as template and the QuickChange Site-Directed Mutagenesis Kit from Stratagene. In-frame fusion of wild-type and mutant RDM1 to the GAL4 transcription-activation domain and the GAL4 DNA-binding domain was carried out using plasmids pGADT7 (*LEU2*) and pGBKT7 (*TRP1*) (BD Biosciences, Clontech), respectively. Constructions were transformed into the host yeast strain AH109, which carries the reporter genes ADE2 and HIS3 driven by GAL4-responsive upstream activation sequences (BD Biosciences, Clontech). Transformants were selected on synthetic dropout agar plates lacking Trp and Leu, and individual colonies were tested for two-hybrid interactions by replica-plating or streaking on plates containing synthetic dropout medium lacking Trp, Leu, His, and Ade (−Trp/−Leu/−His/−Ade).

DNA and RNA substrates. Single- and double-stranded circular ϕX174 DNA was purchased from New England Biolabs. The 52-mer oligonucleotide used in this study (5′-CAAAGTAAGAGCTTCTCGAGCT GCGCAAGGATAGGTCGAATTTTCTCATTTT-3′) is complementary to nucleotides 130–181 of the single-stranded (+) form of ϕX174 DNA. Gel-purified oligonucleotides were purchased from Proligo. DNA and RNA oligonucleotides, as well as *Xho*I-linearized duplex ϕX174 DNA, were 5′-^{32}P-end labeled using polynucleotide kinase and [γ-^{32}P]ATP. Single-stranded ϕX174 DNA was ^{32}P-labeled as described [20]. All DNA and RNA concentrations are expressed in moles of nucleotides.

Expression and purification of wild-type and mutant RDM1. Recombinant chicken RDM1 proteins with an N-terminal, His_6 tag were expressed in *Escherichia coli* using pET15b (Novagen)-based plasmids and purified as described previously [16].

Gel-shift assays. Reactions (20 μl) contained the ^{32}P-labeled DNA or RNA substrates in a standard binding buffer (20 mM MES, pH 6.4, 1 mM DTT). After 5 min at 37 °C, 1 μl of RDM1 protein (or protein diluent (R100 buffer: 20 mM Tris–HCl, pH 8.0, 1 mM EDTA, 0.5 mM DTT, 10% glycerol, and 100 mM KCl) was added and incubation was continued for a further 10 min. Complexes were fixed by addition of glutaraldehyde [final concentration of 0.2% (v/v)] followed by 15 min incubation at 37 °C. Protein–DNA complexes were resolved by electrophoresis through 1% (w/v) agarose gels run in TAE buffer (or in the case of oligonucleotide substrates, 10% polyacrylamide gels in TBE buffer), dried onto filter paper, and visualized by autoradiography.

Binding buffers at pH values ranging from 5.8 to 6.8 (Fig. 3) were generated using 20 mM MES or PIPES. Binding was also tested in more alkaline buffers generated with PIPES, HEPES or triethanolamine–HCl.

Densitometric analysis of the competition gel-shift assays was performed using Scion Image (NIH). Inhibition was calculated based on the percentage of protein complexed over total DNA obtained in the competition reactions, relative to that obtained with no inhibitor present.

Electron microscopy. Binding reactions were fixed by addition of glutaraldehyde to 0.2%, followed by 15 min incubation at 37 °C. Samples were then diluted and washed in 5 mM $Mg(OAc)_2$ before uranyl acetate staining as described [21]. Complexes were observed using a Philips CM100 electron microscope.

DNA fragmentation analysis. Apoptosis was induced in DT40 cells by addition of 50 μM etoposide, and DNA was prepared and analyzed using a published procedure [22].

Results

Binding of RDM1 to DNA and RNA

In previous studies, chicken RDM1 was found to interact with short ssDNA oligonucleotides, resulting in a ladder of protein–DNA complexes, as analyzed by polyacrylamide gel electrophoresis ([16]; see also below). The presence of an RRM prompted us to examine whether RDM1 was also able to bind RNA. To this end, we carried out gel-shift assays using ^{32}P-labeled, 52-mer ssRNA and DNA oligonucleotides of identical sequence. Unlike their counterparts assembled on DNA, RDM1–RNA complexes did not enter polyacrylamide gels (data not shown). Therefore, fixed complexes were analyzed by electrophoresis through 1% agarose gels. Discrete RNA–RDM1 complexes were observed, which varied in mobility and number compared to the shifted DNA–RDM1 complexes (Fig. 1, compare lanes 2–6 with 8–12), probably explaining their different behavior on polyacrylamide gels.

The natural DNA and RNA targets of RDM1 are presently unknown. As a first step to address this question, we analyzed inhibition of DNA binding by the four homopolyribo- and homopolydeoxyribonucleotides. Unlabeled competitors (25-mer ss oligonucleotides) were added at

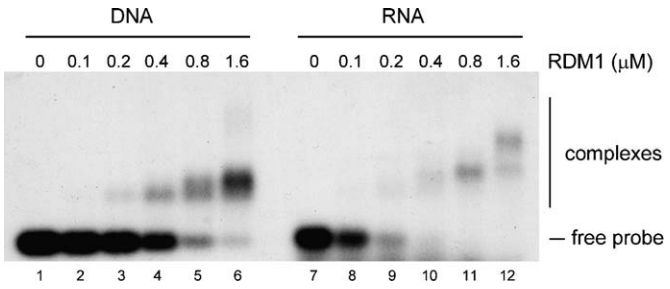

Fig. 1. Binding of RDM1 to DNA and RNA oligonucleotides. The indicated concentrations of RDM1 were incubated with a ^{32}P-labeled 52-mer DNA (lanes 1–6) or RNA (lanes 7–12) oligonucleotide (2 μM). Following fixation with glutaraldehyde, the complexes were analyzed by agarose gel electrophoresis and visualized by autoradiography.

0.1-, 1-, and 10-fold molar excess over a ^{32}P-labeled 52-mer DNA oligonucleotide prior to addition of RDM1. We repeatedly observed that complex formation by RDM1 was largely unaffected by the presence of poly(dA) and poly(dT) (Fig. 2A, lanes 3–5 and 6–8). In contrast, the highest titration points of poly(dC) and poly(dG) in the competition assay nearly eliminated complex formation (Fig. 2A, lanes 11 and 14, 87% and 96% inhibition, respectively), while modest inhibition was already seen at equimolar ratios of competitor over substrate (Fig. 2A, lanes 10 and 13, 7.4% and 13.8% inhibition, respectively).

When homopolyribonucleotides were used to challenge the ssDNA oligonucleotide, poly(G) was found to have an even more inhibitive effect than its deoxynucleotide counterpart, as binding was virtually abolished already in the presence of equimolar amounts of competitors (Fig. 2B, lane 13, 99.5% inhibition). In contrast, poly(C), like poly(U), was found to have little or no effect (Fig. 2B, lanes 6–8 and 9–11). Finally, poly(A) was more inhibitory than poly(dA), showing some degree of inhibition at a 10-fold excess of competitor over substrate (Fig. 2B, lane 5, 33.8% inhibition).

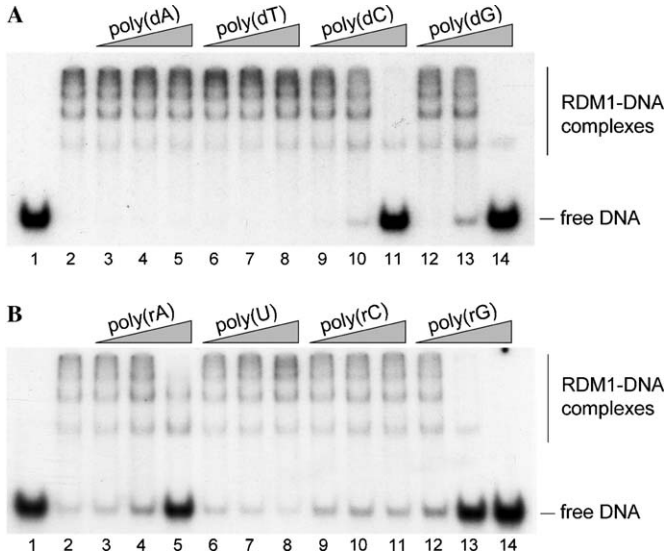

Fig. 2. Competition gel-shift assays. (A) RDM1 (0.75 μM) was incubated with a ^{32}P-labeled 52-mer DNA oligonucleotide (2 μM) and increasing amounts (0.1-, 1-, and 10-fold molar excess) of unlabeled 25-mer homopolydeoxyribonucleotides. Fixed protein–DNA complexes were analyzed by electrophoresis through a 10% polyacrylamide gel and visualized by autoradiography. Lane 2 shows the complexes assembled in the absence of any inhibitor. (B) As described in (A), except that 25-mer homopolyribonucleotides were used.

The effect of pH on the binding of RDM1 to DNA

Preliminary experiments indicated an acidic-pH requirement for RDM1 binding to DNA. We therefore investigated the binding of RDM1 to a ^{32}P-labeled 52-mer oligonucleotide over the pH range 5.8–6.8 in MES- or PIPES-binding buffers (Fig. 3). We found that protein–DNA interactions were enhanced in 20 mM MES, pH 6.4, resulting in complexes that were nicely resolved on polyacrylamide gels (lane 5). Binding efficiency gradually decreased as the pH was increased from 6.4 to 6.8 (lanes 6 and 7). Very little, if any, binding occurred at pH 7.0, and above (data not shown). In contrast, significant aggregation occurred in 20 mM MES, pH 6.2, and this phenomenon increased as the pH was further lowered (lanes 2 and 3). Similar pH effects were observed with plasmid-size ss and dsDNA substrates (data not shown).

Analysis of apoptosis in RDM1$^{-/-}$ mutants

Given that RDM1 interacts with DNA at acidic pH and since acidification is an early event in the apoptotic program that leads to genome degradation [24,25], we tested whether RDM1 may play a role in apoptotic DNA fragmentation. When compared to wild-type DT40 cells, *RDM1*$^{-/-}$ cells appeared to undergo apoptosis normally following exposure to etoposide; no differences were observed in the timing or extent of internucleosomal DNA cleavage (data not shown).

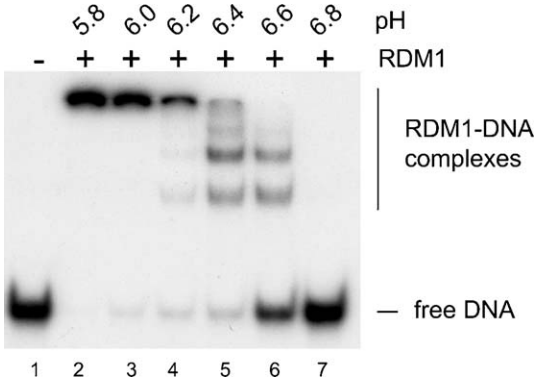

Fig. 3. Effect of pH on RDM1 binding to ssDNA. RDM1 (0.75 μM) was incubated with a ^{32}P-labeled 52-mer DNA oligonucleotide (2 μM) in binding buffers covering the pH range 5.8–6.8, as described under Materials and methods. Fixed complexes were analyzed by polyacrylamide gel electrophoresis and visualized as before. See text for details.

Analysis of the DNA-binding properties of an RDM1 variant mutated in its RD motif using gel-shit assays

RDM1 was initially identified based on a small aa motif, named the RD motif, which is conserved in the RAD52 protein family [16]. Yeast and human RAD52 self-associate to form ring structures that interact with ssDNA and mediate crucial reactions in genetic recombination and DSB repair [17,26–29]. Crystal structure analyses [30,31], together with biochemical and functional analyses of human and yeast RAD52 [19,32], indicate that the RD motif of RAD52 is located in a functionally important region, containing residues involved in ssDNA binding and/or oligomerization. In particular, substitution of AAA for FGY at position 79–81 in HsRAD52 was shown to completely abolish DNA-binding in vitro. Likewise, the single mutations F79A and Y81A afforded no detectable DNA binding [19]. The corresponding positions in RDM1 are well conserved (Fig. 4A). To begin to elucidate the function of the RD motif in chicken RDM1, we therefore examined the DNA-binding properties of a variant containing the AAA for LGF substitution at position 119–121 (Fig. 4A). Gel-shift assays indicated that, compared to wt protein, the RDM1(119–121 LGF → AAA) mutant required a slightly higher concentration to interact with the 52-mer oligonucleotide and resulted in complexes that failed to enter the gel (Fig. 4B). Further DNA-binding assays were performed with ^{32}P-labeled single-stranded and double-stranded ϕX174 DNA. The interaction of wild-type RDM1 protein with circular ssDNA yielded distinct complexes with progressively reduced mobility (Fig. 4C, lanes 1–5), as reported previously [16]. In contrast, the complexes assembled by the mutant protein on ssDNA formed a non-uniform pattern of diffuse bands with variable, often limited, mobility (Fig. 4C, lanes 6–10). In particular, we noted that, at all protein:DNA ratios, part of the labeled DNA was found at the position of the unbound probe. Moreover, certain ratios repeatedly led to the formation of diffuse bands whose front migrated slightly faster than the unbound DNA (see lane 8 for instance), while higher protein concentrations produced a smear extending towards the origin of the gel (lane 10). Taken together, these observations suggested that the RDM1(119–121 LGF → AAA) mutant is affected in its ability to interact with ssDNA. Finally, when assayed using linear duplex ϕX174 DNA, the mutant protein displayed a binding pattern comparable to that described for wild-type RDM1, with the exception that the complexes assembled at the highest concentrations of mutant protein failed to enter the gel (Fig. 4D, compare lanes 4 and 5 with lanes 9 and 10).

Electron microscopic visualization of the complexes assembled by the RDM1(119–121 LGF → AAA) mutant on DNA

In a previous study, we have visualized the interaction between RDM1 and DNA using electron microscopy. On ssDNA, low concentrations of RDM1 led to a uniform distribution of the protein among all the DNA molecules. Higher protein concentrations progressively resulted in denser coating of the DNA and the appearance of small globular aggregates, which formed by aggregation of

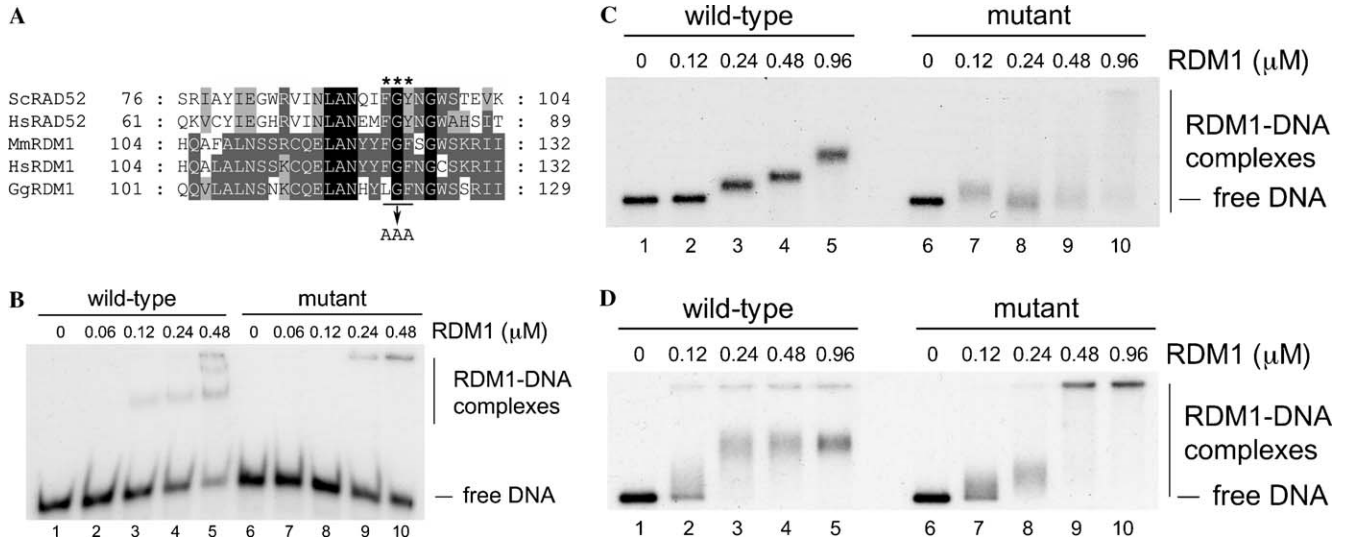

Fig. 4. DNA-binding properties of the RDM1(119–121 LGF → AAA) mutant. (A) Alignment of the RD motif of the RDM1 and RAD52 protein families, showing the position of the LGF → AAA substitution carried out within chicken RDM1, as well as the FGY → AAA substitution in HsRAD52 (asterisks) discussed in the text. Identical residues are highlighted in black. Most conserved residues with a frequency of occurrence >30% are highlighted in gray. Similar residues are shaded in gray. (B) The indicated concentrations of wild-type and mutant protein were incubated with a ^{32}P-labeled 52-mer DNA oligonucleotide (1 μM). Following fixation with glutaraldehyde, protein–DNA complexes were analyzed by PAGE and visualized as before. (C,D) As described for (B), except that the proteins were incubated with 1 μM single-stranded ϕX174 DNA (C) or 0.5 μM linear duplex ϕX174 DNA (D), and complexes were analyzed by agarose gel electrophoresis.

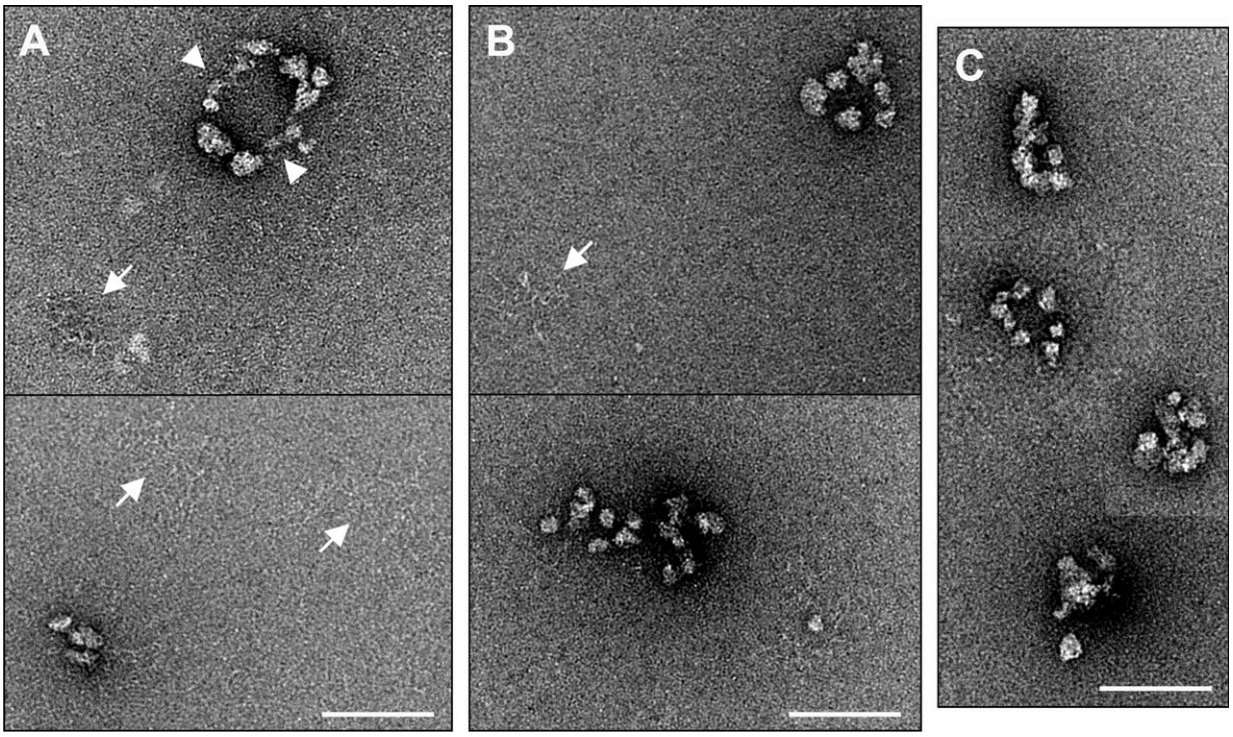

Fig. 5. Electron microscopic visualization of complexes assembled by RDM1(119–121 LGF → AAA) on single-stranded DNA. Reactions contained ϕX174 circular ssDNA (1 μM) and the following concentrations of protein: 30 nM (A), 60 nM (B), and 240 nM (C). Arrows point to unbound, collapsed ssDNA. Arrowheads point to RDM1-covered regions that assemble into higher-order, globular structures. Complexes were fixed with glutaraldehyde and visualized after negative staining. (C) Composite image formed with several complexes observed in different fields. See text for details. The magnification bars denote 100 nm.

RDM1–ssDNA complexes [16]. When examined by electron microscopy, ssDNA-binding reactions containing the RDM1(119–121 LGF → AAA) variant revealed its unequal distribution among the DNA molecules, as illustrated by the simultaneous presence of unbound ssDNA, visible as tangles of collapsed molecules, and DNA complexed with various amounts of protein (Figs. 5A and B). Extensively bound DNA molecules could already be observed in reactions containing 30 nM mutant protein (Fig. 5A, upper panel). In support of the gel-shift data, these observations suggest that, unlike wild-type protein, the RDM1(119–121 LGF → AAA) mutant displays some degree of cooperativity in binding to ssDNA. Nonetheless, the complexes assembled by the mutant protein resembled those formed at high concentrations of wild-type RDM1, as they consisted in small globular aggregates probably originating from protein-coated ssDNA regions, which were still visible on some complexes (Fig. 5). In view of the extensive binding afforded by the mutant protein, it is surprising that, over a large protein concentration range, the complexes formed by the mutant protein displayed smaller shifts in mobility than those of wild-type RDM1 (Fig. 4C). A likely explanation, provided by studies of DNA binding by histone H1 [33], is that the triple mutation results in conformational changes which affect the extent of glutaraldehyde-mediated charge neutralization of the complexes and hence their electrophoretic mobility. Finally, analysis of the complexes formed by the RDM1(119–121 LGF → AAA) variant in the presence of duplex DNA revealed the formation of filament-like structures similar to those described for the wild-type protein (Fig. 6) [16], consistent with the gel-shift data.

Homotypic interactions of RDM1

The assembly of filament-like structures on dsDNA prompted us to monitor homotypic protein–protein interactions of RDM1 using the yeast two-hybrid assay. Full-length wild-type and mutant RDM1(119–121 LGF → AAA) were fused to the GAL4 transcription-activation domain (pGADT7) or DNA binding domain (pGBKT7) and transformed into yeast strain AH109. The constructs showed no self-activation of the reporter genes when assayed on selective medium (Leu^-, Trp^-, His^-, and Ade^-) (Fig. 7). In contrast, homotypic interactions of both wild-type RDM1 and RDM1(119–121 LGF → AAA) were detected on this medium (Fig. 7), in agreement with the gel-shifts and electron microscopy data.

Discussion

We have previously reported that RDM1 interacts with ss- and dsDNA in vitro, resulting in filament-like structures and other higher-order structures that might reflect a

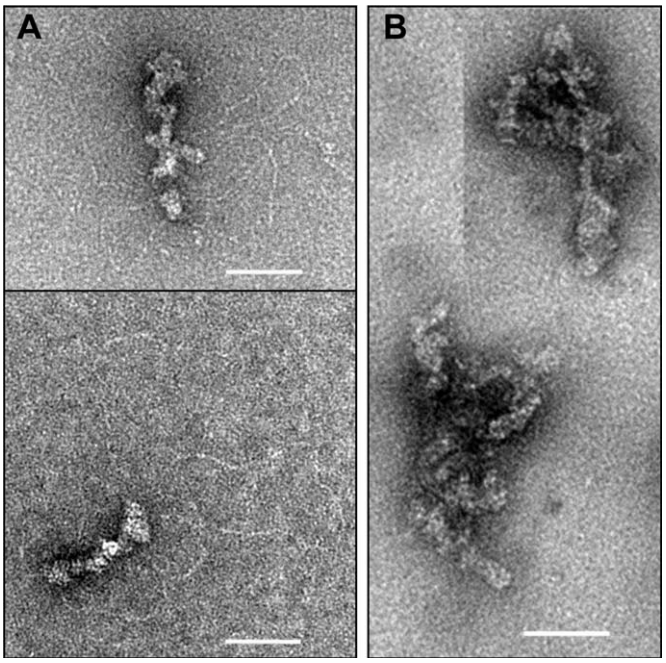

Fig. 6. Electron microscopic visualization of complexes assembled by RDM1(119–121 LGF → AAA) on double-stranded DNA. Reactions contained linear duplex ϕX174 DNA (0.5 μM) and 60 nM (A) or 240 nM (B) protein. (B) Composite image formed with complexes observed in the same field. The magnification bars denote 60 nm.

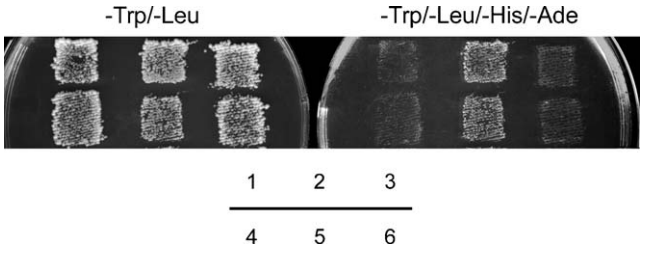

Fig. 7. Yeast two-hybrid analysis of RDM1 homotypic interactions. pGADT7 (*LEU2*) and pGBKT7 (*TRP1*) vectors expressing the following constructions of RDM1 were transformed into AH109 and tested for two-hybrid interactions by replica-plating on −Trp/−Leu/−His/−Ade plates: 1, pGADT7 + pGBKT7-RDM1(A_{119}AA); 2, pGADT7-RDM1(A_{119}AA) + pGBKT7-RDM1(A_{119}AA); 3, pGADT7-RDM1(A_{119}AA) + pGBKT7; 4, pGADT7 + pGBKT7-RDM1; 5, pGADT7-RDM1 + pGBKT7-RDM1; 6, pGADT7-RDM1 + pGBKT7. Pictures were taken 48 h after replica-plating. See text for details.

dynamic role in the context of chromatin [16]. As expected from the presence of an RRM, we have now shown that RDM1 can bind to RNA as well as DNA. RDM1 can therefore be added to the list of RRM-containing proteins capable of associating with RNA and DNA [6–9,11]. Furthermore, our data from competition gel-shift assays suggest that RDM1 is capable of discrimination between the two nucleic acids. Thus, the purine bases G and, to a lesser extent, A, were efficient inhibitors of DNA binding when present as homopolyribonucleotides, while the pyrimidine poly(C) and poly(U) had no effect. In contrast, no base bias was observed with polydeoxyribonucleotides as poly(dG) and poly(dC) were found to achieve almost equal inhibition, while poly(dA) and poly(dT) had no effect. We noted also that poly(G) was a much more efficient inhibitor than poly(dG). We are currently carrying out experiments to identify the biological nucleic acid targets of RDM1.

While RDM1 displays very little DNA-binding activity at pH 6.8, or above, its interaction with DNA was enhanced at more acidic pHs. This observation suggests that RDM1 might function in acidic cellular contexts. Acidic pH plays a critical role in processes that affect cell survival, drug resistance, DNA repair, and tumorigenesis [34,35]. Low pH has been shown to enhance the DNA-binding activity of the transcription factor Sp1, as well as its interaction with TATA-binding protein, and it has been postulated that such modulation may provide an advantage in the context of cellular acidosis [36]. The physiological relevance of the acidic pH-dependent DNA-binding activity of RDM1 remains to be determined.

Based on studies of the RAD52 protein, we have previously hypothesized that the RD motif of RDM1 may contribute to its DNA-binding activity, possibly as a modulator of its RRM [16]. Mutational analysis of human RAD52 protein has shown that DNA-binding activity is abolished in the (79–81 FGY → AAA) mutant as well as in the single mutants F79A and Y81A, and it has been suggested that these residues are in direct contact with ssDNA [19]. The triple alanine substitution (119–121 LGF → AAA) within the RD motif of RDM1 still affords binding to both ss- and dsDNA, consistent with the presence of an intact RRM as the major determinant of the DNA-binding activity of RDM1. Moreover, this mutation did not compromise the self-interaction of RDM1 as analyzed by the yeast two-hybrid system, gel-shift assays, and electron microscopy. However, the L_{119}GF → AAA mutation was found to affect the ssDNA-binding properties of RDM1, leading to anomalous binding to oligonucleotides and imparting some degree of cooperativity of binding in the presence of ϕX174 ssDNA, as illustrated by the simultaneous presence of unbound and extensively bound DNA molecules in reactions containing low concentrations of protein. Previously, we have shown that the addition of small amounts of RDM1 protein to plasmid-size DNA led to its uniform distribution among the DNA molecules, consistent with a non-cooperative model comprising independent binding sites [16]. Our data indicate that this mode of binding is altered by the L_{119}GF → AAA mutation. The observations reported here may reflect a role for the domain identified by this mutation at the protein–ssDNA and/or protein–protein interfaces. An attractive hypothesis is that this domain contributes additional nucleic acid-binding surface and properties to the RRM. Situations where the binding surface provided by a single RRM is enlarged through the contribution of additional amino acids are well documented [1,37]. Whether residues of the L_{119}GF sequence make direct contact with DNA or play a more structural role

remains to be determined. Likewise, further work is required to delineate the domain involved in the modulation of RDM1 mode of interaction with ssDNA, and determine the extent to which it may overlap with the RD motif.

Acknowledgments

We are very grateful to Pierre Hainaut and Jacques Dubochet for their interest and support. We thank Georges Mollon for his assistance during preparation of the figures.

References

[1] C. Maris, C. Dominguez, F.H. Allain, The RNA recognition motif, a plastic RNA-binding platform to regulate post-transcriptional gene expression, FEBS J. 272 (2005) 2118–2131.
[2] A. Bateman, E. Birney, L. Cerruti, R. Durbin, L. Etwiller, S.R. Eddy, S. Griffiths-Jones, K.L. Howe, M. Marshall, E.L. Sonnhammer, The Pfam protein families database, Nucleic Acids Res. 30 (2002) 276–280.
[3] M.S. Swanson, T.Y. Nakagawa, K. LeVan, G. Dreyfuss, Primary structure of human nuclear ribonucleoprotein particle C proteins: conservation of sequence and domain structures in heterogeneous nuclear RNA, mRNA, and pre-rRNA-binding proteins, Mol. Cell Biol. 7 (1987) 1731–1739.
[4] E. Birney, S. Kumar, A.R. Krainer, Analysis of the RNA-recognition motif and RS and RGG domains: conservation in metazoan pre-mRNA splicing factors, Nucleic Acids Res. 21 (1993) 5803–5816.
[5] H. Ginisty, F. Amalric, P. Bouvet, Two different combinations of RNA-binding domains determine the RNA binding specificity of nucleolin, J. Biol. Chem. 276 (2001) 14338–14343.
[6] F. Ishikawa, M.J. Matunis, G. Dreyfuss, T.R. Cech, Nuclear proteins that bind the pre-mRNA 3′ splice site sequence r(UUAG/G) and the human telomeric DNA sequence d(TTAGGG)n, Mol. Cell Biol. 13 (1993) 4301–4310.
[7] K. Moran-Jones, L. Wayman, D.D. Kennedy, R.R. Reddel, S. Sara, M.J. Snee, R. Smith, hnRNP A2, a potential ssDNA/RNA molecular adapter at the telomere, Nucleic Acids Res. 33 (2005) 486–496.
[8] E.A. Suswam, Y.Y. Li, H. Mahtani, P.H. King, Novel DNA-binding properties of the RNA-binding protein TIAR, Nucleic Acids Res. 33 (2005) 4507–4518.
[9] D.J. De Angelo, J. De Falco, L. Rybacki, G. Childs, The embryonic enhancer-binding protein SSAP contains a novel DNA-binding domain which has homology to several RNA-binding proteins, Mol. Cell Biol. 15 (1995) 1254–1264.
[10] S.D. Johnston, J.E. Lew, J. Berman, Gbp1p, a protein with RNA recognition motifs, binds single-stranded telomeric DNA and changes its binding specificity upon dimerization, Mol. Cell Biol. 19 (1999) 923–933.
[11] A. Basu, B. Dong, A.R. Krainer, C.C. Howe, The intracisternal A-particle proximal enhancer-binding protein activates transcription and is identical to the RNA- and DNA-binding protein p54nrb/NonO, Mol. Cell Biol. 17 (1997) 677–686.
[12] E.P. Newberry, T. Latifi, D.A. Towler, The RRM domain of MINT, a novel Msx2 binding protein, recognizes and regulates the rat osteocalcin promoter, Biochemistry 38 (1999) 10678–10690.
[13] M. Samuels, G. Deshpande, P. Schedl, Activities of the sex-lethal protein in RNA binding and protein:protein interactions, Nucleic Acids Res. 26 (1998) 2625–2637.
[14] V.N. Kim, G. Dreyfuss, Nuclear mRNA binding proteins couple pre-mRNA splicing and post-splicing events, Mol. Cells 12 (2001) 1–10.
[15] S.J. Kavanagh, T.C. Schulz, P. Davey, C. Claudianos, C. Russell, P.D. Rathjen, A family of RS domain proteins with novel subcellular localization and trafficking, Nucleic Acids Res. 33 (2005) 1309–1322.
[16] S. Hamimes, H. Arakawa, A.Z. Stasiak, A.M. Kierzek, S. Hirano, Y.G. Yang, M. Takata, A. Stasiak, J.M. Buerstedde, E. Van Dyck, RDM1, a novel RNA recognition motif (RRM)-containing protein involved in the cell response to cisplatin in vertebrates, J. Biol. Chem. 280 (2005) 9225–9235.
[17] S.C. West, Molecular views of recombination proteins and their control, Nat. Rev. Mol. Cell Biol. 4 (2003) 435–445.
[18] M. van den Bosh, P.H. Lohman, A. Pastink, DNA double-strand break repair by homologous recombination, Biol. Chem. 383 (2002) 873–892.
[19] J.A. Lloyd, D.A. McGrew, K.L. Knight, Identification of residues important for DNA binding in the full-length human Rad52 protein, J. Mol. Biol. 345 (2005) 239–249.
[20] E. Van Dyck, N.M. Hajibagheri, A. Stasiak, S.C. West, Visualisation of human Rad52 protein and its complexes with hRad51 and DNA, J. Mol. Biol. 284 (1998) 1027–1038.
[21] J. Sogo, A. Stasiak, W. DeBernardin, R. Losa, R.T. Koller, Electron Microscopy in Molecular Biology, in: J. Sommerville, U. Scheer (Eds.), IRL Press at Oxford University Press, Oxford, 1987, pp. 61–79.
[22] S. Ruchaud, N. Korfali, P. Villa, T.J. Kottke, C. Dingwall, S.H. Kaufmann, W.C. Earnshaw, Caspase-6 gene disruption reveals a requirement for lamin A cleavage in apoptotic chromatin condensation, EMBO J. 21 (2002) 1967–1977.
[23] F. Dallaire, S. Dupuis, S. Fiset, B. Chabot, Heterogeneous nuclear ribonucleoprotein A1 and UP1 protect mammalian telomeric repeats and modulate telomere replication in vitro, J. Biol. Chem. 275 (2000) 14509–14516.
[24] S. Nagata, DNA degradation in development and programmed cell death, Annu. Rev. Immunol. 23 (2005) 853–875.
[25] J. Li, A. Eastman, Apoptosis in an interleukin-2-dependent cytotoxic T lymphocyte cell line is associated with intracellular acidification. Role of the Na(+)/H(+)-antiport, J. Biol. Chem. 270 (1995) 3203–3211.
[26] W. Kagawa, H. Kurumizaka, S. Ikawa, S. Yokoyama, T. Shibata, Homologous pairing promoted by the human Rad52 protein, J. Biol. Chem. 276 (2001) 35201–35208.
[27] A.Z. Stasiak, E. Larquet, A. Stasiak, S. Muller, A. Engel, E. Van Dyck, S.C. West, E.H. Egelman, The human Rad52 protein exists as a heptameric ring, Curr. Biol. 10 (2000) 337–340.
[28] E. Van Dyck, A.Z. Stasiak, A. Stasiak, S.C. West, Binding of double-strand breaks in DNA by human Rad52 protein, Nature 398 (1999) 728–731.
[29] C.A. Parsons, P. Baumann, E. Van Dyck, S.C. West, Precise binding of single-stranded DNA termini by human RAD52 protein, EMBO J. 19 (2000) 4175–4181.
[30] W. Kagawa, H. Kurumizaka, R. Ishitani, S. Fukai, O. Nureki, T. Shibata, S. Yokoyama, Crystal structure of the homologous-pairing domain from the human Rad52 recombinase in the undecameric form, Mol. Cell 10 (2002) 359–371.
[31] M.R. Singleton, L.M. Wentzell, Y. Liu, S.C. West, D.B. Wigley, Structure of the single-strand annealing domain of human RAD52 protein, Proc. Natl. Acad. Sci. USA 99 (2002) 13492–13497.
[32] U.H. Mortensen, N. Erdeniz, Q. Feng, R. Rothstein, A molecular genetic dissection of the evolutionarily conserved N terminus of yeast Rad52, Genetics 161 (2002) 549–562.
[33] W. De Bernardin, R. Losa, T. Koller, Formation and characterization of soluble complexes of histone H1 with supercoiled DNA, J. Mol. Biol. 189 (1986) 503–517.
[34] P. Wong, C. Lee, I.F. Tannock, Reduction of intracellular pH as a strategy to enhance the pH-dependent cytotoxic effects of melphalan for human breast cancer cells, Clin. Cancer Res. 11 (2005) 3553–3557.
[35] M. Stubbs, P.M. McSheehy, J.R. Griffiths, C.L. Bashford, Causes and consequences of tumour acidity and implications for treatment, Mol. Med. Today 6 (2000) 15–19.

[36] T. Torigoe, H. Izumi, Y. Yoshida, H. Ishiguchi, T. Okamoto, H. Itoh, K. Kohno, Low pH enhances Sp1 DNA binding activity and interaction with TBP, Nucleic Acids Res. 31 (2003) 4523–4530.

[37] L. Volpon, I. D'Orso, C.R. Young, A.C. Frasch, K. Gehring, NMR structural study of TcUBP1, a single RRM domain protein from *Trypanosoma cruzi*: contribution of a beta hairpin to RNA binding, Biochemistry 44 (2005) 3708–3717.